

Article

Impact of Spatial Resolution on Wind Field Derived Estimates of Air Pressure Depression in the Hurricane Eye

Ruba Amarin ^{1,*}, Christopher Ruf ² and Linwood Jones ¹

¹ Central Florida Remote Sensing Lab., School of Electrical Engineering and Computer Science, University of Central Florida, Box-162450, Orlando, FL 32816-2450, USA; E-Mail: ljones5@cfl.rr.com

² Space Physics Research Laboratory, College of Engineering, University of Michigan, 2455 Hayward Street, Ann Arbor, MI 48109, USA; E-Mail: cruf@umich.edu

* Author to whom correspondence should be addressed; E-Mail: ramarin@mail.ucf.edu; Tel.: +1-321-750-9542; Fax: +1-321-868-1035.

Received: 8 December 2009; in revised form: 8 February 2010 / Accepted: 25 February 2010 /

Published: 1 March 2010

Abstract: Measurements of the near surface horizontal wind field in a hurricane with spatial resolution of order 1–10 km are possible using airborne microwave radiometer imagers. An assessment is made of the information content of the measured winds as a function of the spatial resolution of the imager. An existing algorithm is used which estimates the maximum surface air pressure depression in the hurricane eye from the maximum wind speed. High resolution numerical model wind fields from Hurricane Frances 2004 are convolved with various HIRAD antenna spatial filters to observe the impact of the antenna design on the central pressure depression in the eye that can be deduced from it.

Keywords: HIRAD; hurricane winds; pressure; spatial resolution; filters

1. Introduction

The Hurricane Imaging Radiometer (HIRAD) is a next-generation airborne microwave remote sensor under development by NASA, which will expand the airborne hurricane measuring capabilities of two existing microwave radiometers—the Stepped Frequency Microwave Radiometer (SFMR) [1] and the Lightweight Rainfall Radiometer (LRR) [2]. HIRAD combines the multi-frequency C-band channels of the real aperture SFMR with the pushbroom surface imaging capabilities of the LRR Synthetic Thinned Array Radiometer (STAR) to produce wide-swath imagery of the near surface wind

speed and rain rate in and near a hurricane. The HIRAD swath width extends to approximately three-times the aircraft altitude and, at an altitude of 20 km; its spatial resolution varies between 0.6 and 3 km depending on channel frequency and swath position. The swath for a typical HIRAD pass through the eye (with the aircraft at 20 km) would extend to cover the full eyewall region of a strong compact storm. Because of its wide-swath, high resolution imaging capability, HIRAD provides the opportunity to examine the detailed structure of the near surface (10 m height) wind field [3]. In particular, we consider the information contained in the wind field and its dependence on the spatial resolution of the image. In Section 2, an algorithm is described which estimates the minimum air pressure in the hurricane eye using the wind field. Air pressure depression is a fundamental indicator of the current and potential future strength of a hurricane. In Section 3, the algorithm is applied to a highly resolved, physically based numerical hurricane model, which provides a realistic representation of the variability of the wind field on spatial scales that are resolvable by HIRAD. Simulated HIRAD retrievals with variable spatial resolution of the surface wind field are derived from the high resolution numerical hurricane model, and the impact of reduced spatial resolution on the ability to accurately estimate the air pressure in the hurricane eye is assessed.

2. Pressure Depression Estimator

The pressure depression estimator is based on previous work by Holland [4] that is summarized and adapted here. According to Holland, the pressure, p , at radius, r , is approximated by

$$p = p_c + (p_n - p_c) \exp(-A/r^B) \quad (1)$$

where p_c is the central pressure, p_n is the ambient pressure (theoretically at infinite radius) and A and B are scaling parameters. Holland also computed the maximum wind speed according to

$$V_m = C(p_n - p_c)^{1/2} \quad (2)$$

where

$$C = (B/\rho e)^{1/2} \quad (3)$$

The parameter B in (1) defines the shape of the profile and A determines its location relative to the origin. The value of B lies between 1 and 2.5 and is assumed to be 1 for this study. ρ in (3) is the air density and is assumed constant at 1.15 kg/m^3 [4] and e is the base of natural logarithms. The maximum wind speed equation has been used widely for estimating the maximum winds in hurricanes.

In the following analysis, $p_n = 1,013 \text{ mbar}$ is assumed far from the hurricane. This is the nominal background pressure and is consistent with the fact that Holland considers the “infinite” radius location to be far from the hurricane center [4]. Note that the model used here assumes cyclostrophic balance, in which the Coriolis force can be ignored in the region of maximum winds and there is assumed to be a balance between the centrifugal and pressure forces [5].

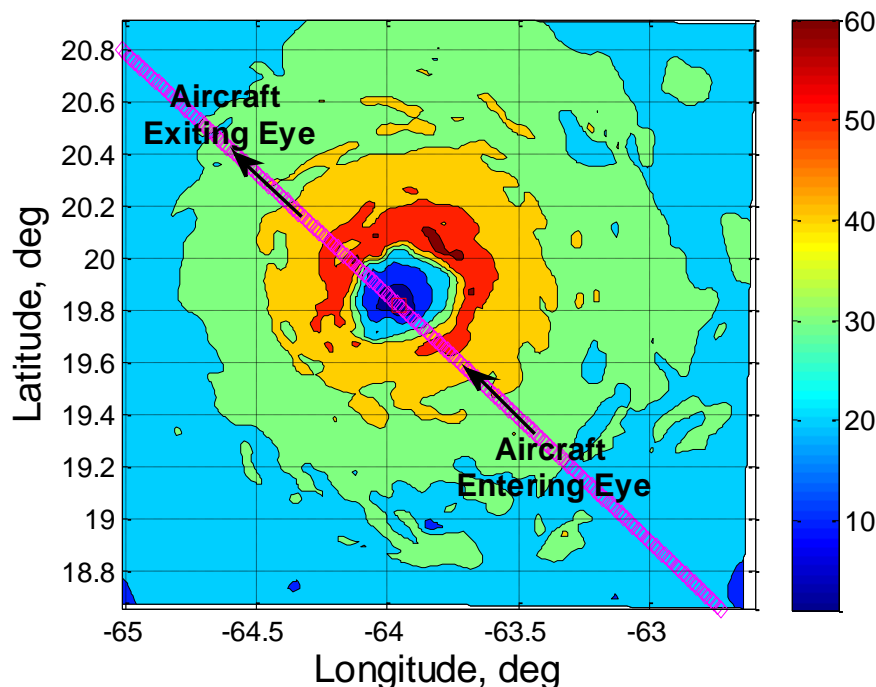
We emphasize that this pressure depression estimation algorithm is based on a very simplified model for the hurricane. It is not presented as an accurate means of deriving actual air pressure depression values in the hurricane eye in an operational setting. Rather, our intent with this pressure depression estimator is to provide a quantitative relative assessment of the information contained in measured wind fields as a function of their spatial resolution. We focus in particular on our ability to

estimate pressure depression as a measure of information content because of the considerable historical interest in its determination in tropical cyclones [6].

3. Application to a Simulated Hurricane

A simulated hurricane wind field (Figure 1) was used in this study which was derived from observations made of Hurricane Frances on 31 August 2004 using a dynamical numerical model described by Chen [7]. The Chen model is non-hydrostatic with detailed explicit microphysics and an interactive ocean wave model that uses a system of nested grids with the innermost one having a grid spacing of 0.015 degrees (1.67 km) in longitude and latitude. The model produces a realistic 3D representation of hurricane environmental parameters that includes an eyewall, rainbands and other typical convective and mesoscale structures. A northeast-to-southwest aircraft transect (indicated in magenta in Figure 1) was used in this analysis. Along this ground track, which will be the nadir pixel of the HIRAD swath, the maximum wind speed value is ~60 m/s, at a radial distance of ~25.7 km from the eye center.

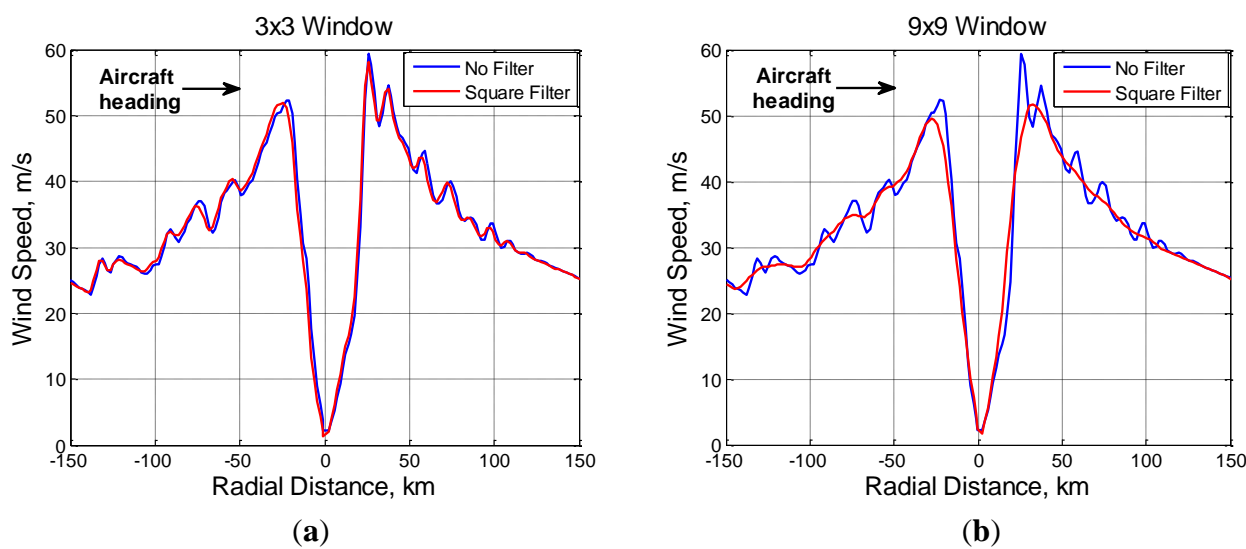
Figure 1. Hurricane Frances wind field on 31 August, 2004 with wind speed (m/s) represented by the filled-contours colorscale. The aircraft ground track is shown as the solid (magenta) line.



A variety of running average spatial filters was applied to the U and V components of the original wind field, thereby producing a new, filtered, wind field that reproduces the impact of spatial smoothing by the HIRAD antenna pattern. A square filter with window sizes of 3×3 , 5×5 , 7×7 and 9×9 pixels was applied to produce a “box-car” simulation of the HIRAD antenna pattern with variable beamwidth. For example, the 3×3 filtered image would have a resolution of 3×1.67 km. For each filtered image, the pressure depression estimator was applied to the wind field. The first processing step of the estimator is the determination of the maximum wind speed value for the

specified resolution. Next, the maximum wind speed value is used in (2) to estimate the minimum air pressure in the hurricane eye. With degraded resolution, the ability to resolve the peak wind is degraded, as is the estimate of the minimum air pressure in the hurricane eye. Figure 2 shows line plots of the wind speed along the ground track for a 3×3 and 9×9 window sizes, along with the original, unfiltered, wind for comparison.

Figure 2. The ground track wind speed for: (a) 3×3 and (b) 9×9 square spatial filter windows (shown in red) and the unfiltered wind (blue).

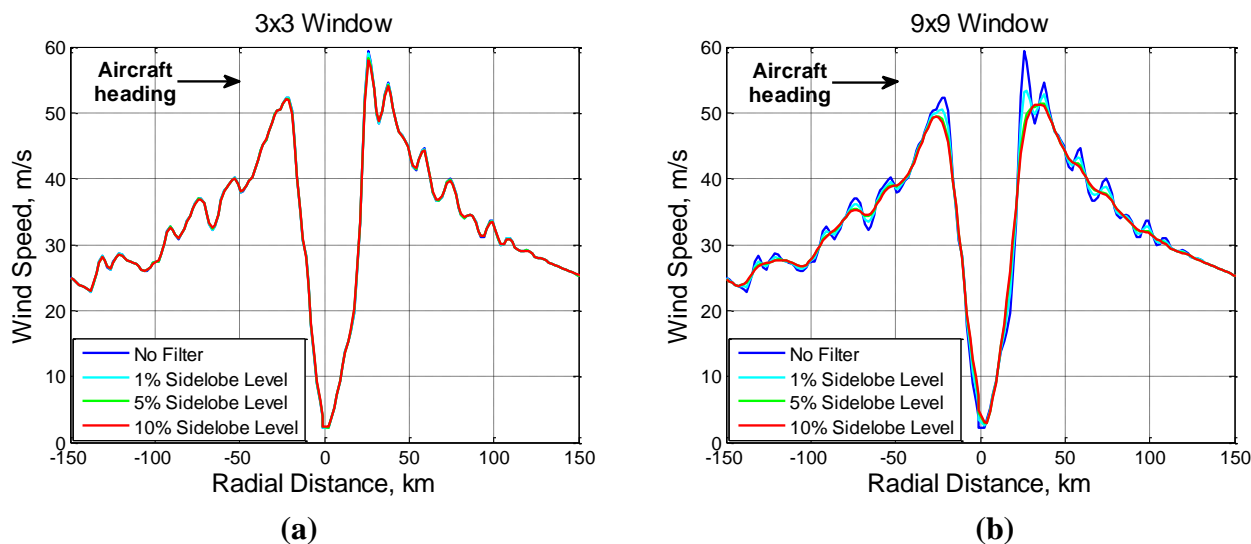


The magnitude of the wind speed decreases as the window filter size increases, which represents the spatial smoothing, or resolution degradation, caused by increasing the size of the antenna footprint. The maximum wind speed value reported for a 3×3 window is 58 m/s while for a 9×9 window the value is 51.7 m/s. These values are used to compute a pressure estimate inside the eyewall region, and the results are given in Table 1.

Another idealized spatial filter that was considered is the “top hat”. This is a running average window in which the central (1×1 pixel) portion has unity gain and the remainder of the window is a smaller constant value. This filter is a more realistically model for the antenna sidelobe structure of the HIRAD imager. The sidelobe level was set equal to 1%, 5% and 10% of the magnitude of the central top hat portion, which corresponds to three different antenna beam efficiencies for the various spatial filter sizes.

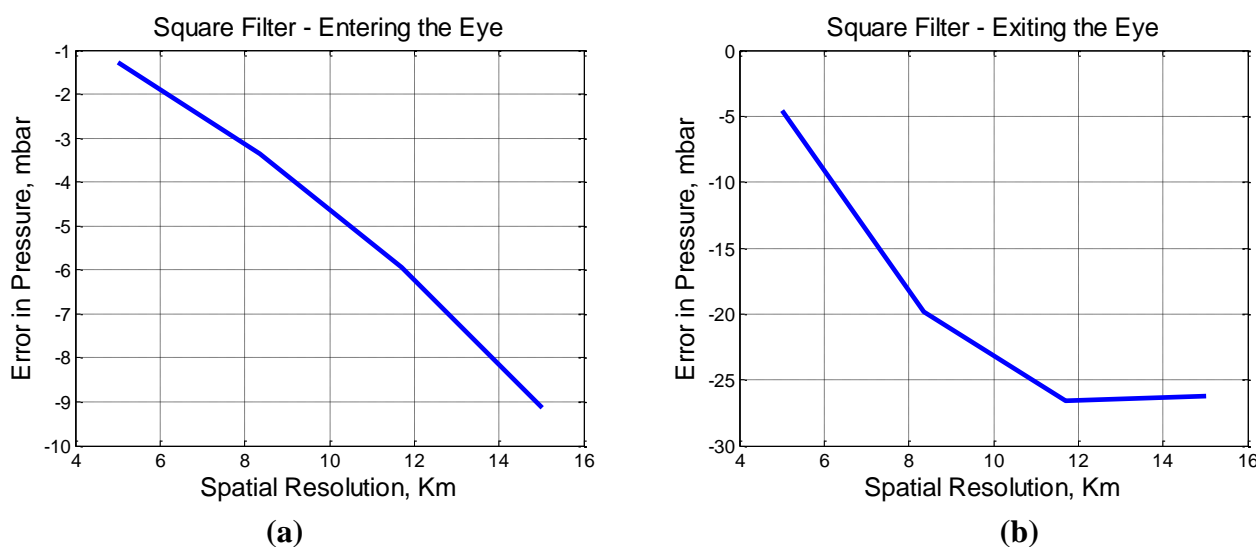
The objective of this simulation is to assess the impacts of antenna beam width and sidelobe level on the derived wind field products. Figure 3 contains the ground track wind speed for 3×3 and 9×9 window sizes and for three different sidelobe levels, along with the unfiltered wind speed. For a 3×3 window, results show that there is not a significant difference in the computed wind speed between the three different sidelobe levels; whereas, for a 9×9 window, the 10% sidelobe level has the maximum degrading effect on the computed wind speed. Values of the maximum wind speed (in m/s) are also given in Table 2.

Figure 3. The ground track wind speed for: (a) 3×3 and (b) 9×9 “top hat” filter windows for different sidelobe levels (shown in different colors) and the unfiltered wind (blue).



The pressure inside the eye can be calculated from the maximum wind speed values for each window size for both filters. This was performed for the aircraft transect shown in Figure 1. Figure 4 shows the error in the pressure depression estimate as a function of spatial resolution on each side of the eyewall. In the figure, the 3×3 , 5×5 , 7×7 and 9×9 window sizes correspond to 5.01, 8.35, 11.69 and 15.03 km spatial resolution, respectively.

Figure 4. Error in the pressure depression estimate as a function of spatial resolution for (a) entering the eye and (b) exiting the eye region.



Results show a continuous increase in the magnitude of the pressure error as the spatial resolution degrades. The dramatic increase in error for the 9×9 window relative to the 3×3 case is due to the averaging, or spatial smoothing, of the wind field over the larger HIRAD footprint.

Figure 5. Error in the pressure depression estimation as a function of antenna beam efficiency for (a) entering the eye and (b) exiting the eye region.

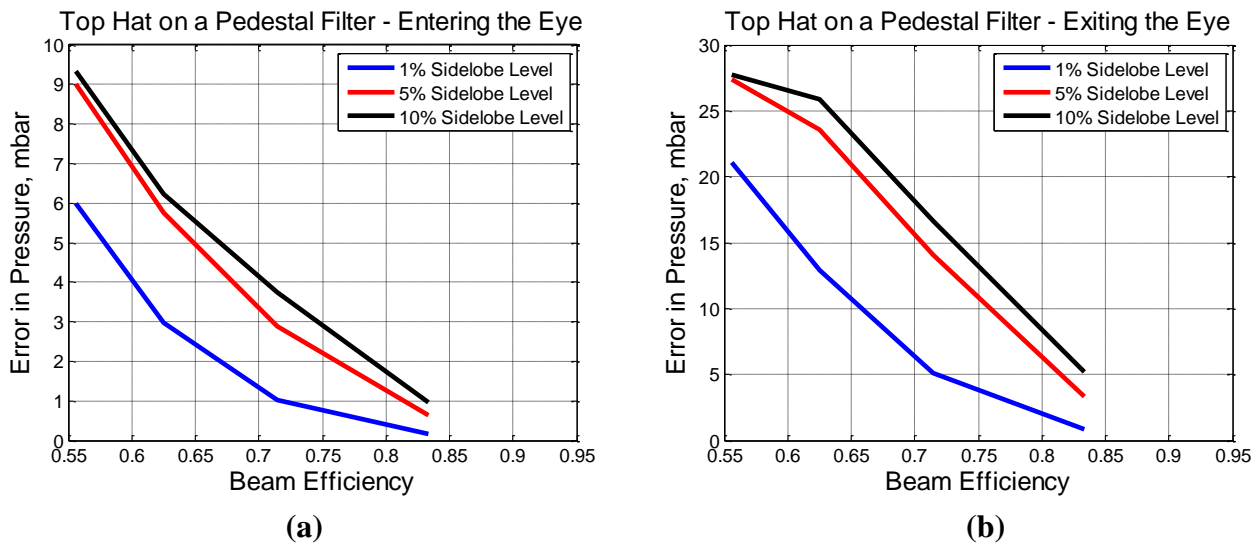


Figure 5 shows the error in the pressure depression estimate as a function of beam efficiency for the “top hat” filter on each side of the eyewall. Results show that the error in pressure is smaller for the 1% sidelobe level filter and that errors increase with the magnitude of the side lobe level (*i.e.*, decreasing antenna beam efficiency). The error in estimates of the radial distance of the peak wind from the hurricane eye was also computed as a function of beam efficiency. Results showed a smaller difference on the entering side, while there is a maximum error of 10.02 km (6 pixels) on the exiting side. Typical microwave radiometer antennas are designed for a beam efficiency of 90% or greater, which would not contribute significant error according to these results. HIRAD offers a trade-off between beam efficiency and swath width that might be exploited, but with these results in mind, Tables 1 and 2 summarize these results.

Table 1. Pressure depression for box-car filters of varying spatial resolution.

| Parameters | | No Filter | Square Filter | | | |
|--------------|-----------------------|-----------|---------------|-------|-------|-------|
| | | | 3 × 3 | 5 × 5 | 7 × 7 | 9 × 9 |
| Entering Eye | Max. Wind Speed (m/s) | 52.35 | 51.96 | 51.32 | 50.51 | 49.48 |
| | Radial Distance (km) | 22.68 | 24.35 | 26.02 | 26.02 | 27.69 |
| | Pressure (mbar) | 927.28 | 928.5 | 930.6 | 933.2 | 936.4 |
| Exiting Eye | Max. Wind Speed (m/s) | 59.3 | 58.06 | 53.69 | 51.64 | 51.74 |
| | Radial Distance (km) | 25.75 | 25.75 | 25.75 | 30.76 | 32.43 |
| | Pressure (mbar) | 903.0 | 907.5 | 922.8 | 929.6 | 929.3 |

Table 2. Pressure depression for top-hat filters of varying spatial resolution and sidelobe levels.

| Parameter | | Top Hat Filter | | | | | | | | | | | |
|--------------|-----------------------|----------------|-------|-------|-------|-------|-------|-------|-------|-------|-------|-------|-------|
| | | 1% | | | | 5% | | | | 10% | | | |
| | | 3 × 3 | 5 × 5 | 7 × 7 | 9 × 9 | 3 × 3 | 5 × 5 | 7 × 7 | 9 × 9 | 3 × 3 | 5 × 5 | 7 × 7 | 9 × 9 |
| Entering Eye | Max. Wind Speed (m/s) | 52.30 | 52.03 | 51.43 | 50.49 | 52.16 | 51.46 | 50.56 | 49.52 | 52.05 | 51.20 | 50.41 | 49.41 |
| | Radial Distance (km) | 22.68 | 22.68 | 22.68 | 22.68 | 22.68 | 22.68 | 24.35 | 26.02 | 22.68 | 22.68 | 24.35 | 26.02 |
| | Pressure (mbar) | 927.4 | 928.3 | 930.3 | 933.3 | 927.9 | 930.2 | 933.0 | 936.3 | 928.3 | 931.0 | 933.5 | 936.6 |
| Exiting Eye | Max. Wind Speed (m/s) | 59.07 | 57.91 | 55.70 | 53.31 | 58.40 | 55.39 | 52.57 | 51.38 | 57.89 | 54.63 | 51.85 | 51.27 |
| | Radial Distance (km) | 25.75 | 25.75 | 25.75 | 27.42 | 25.75 | 25.75 | 27.42 | 35.77 | 25.75 | 27.42 | 29.09 | 34.10 |
| | Pressure (mbar) | 903.9 | 908.1 | 915.9 | 924.1 | 906.3 | 917.0 | 926.6 | 930.4 | 908.2 | 919.6 | 928.9 | 930.8 |

4. Summary

An algorithm has been used which estimates the minimum air pressure in the central eye region of a hurricane from its wind field. The estimator computes the maximum value of the winds, and the central air pressure depression is derived from the maximum wind speed value. The wind fields are simulated by a physically-based, dynamical numerical model that faithfully represents the expected spatial variability of an actual hurricane wind field. This algorithm is applied to simulated hurricane wind fields as measured by HIRAD with varying antenna spatial resolution and sidelobe structure.

Different HIRAD antenna spatial filters were used to simulate various antenna pattern characteristics. Generally, either degrading the spatial resolution or decreasing the beam efficiency will cause an underestimation of the maximum winds, which in turn will cause the minimum pressure to be over estimated. Errors in pressure due to low antenna beam efficiency were found to be relatively small (approximately 8 mbar or less) for beam efficiency values of approximately 80% or higher. Errors due to degraded spatial resolution (worse than the 1.67 km value that is achievable by HIRAD from aircraft altitudes) were found to range from approximately 5 mbar with 4 km resolution to greater than 20 mbar at 15 km resolution. These results suggest that spatial resolution of a few km or better is required to estimate minimum pressure in the hurricane eye to better than 5 mbar. The pressure depression estimator has been applied in this work to a single hurricane model as an example of its use in estimating the information content of a hurricane wind field as a function of its spatial resolution. A more complete study of the relationship between spatial resolution and information content should consider hurricanes of varying sizes and strengths. This is a subject for future work.

References and Notes

1. Uhlhorn, E.W.; Black, P. G.; Franklin, J.L.; Goldstein, A.S. Hurricane Surface Wind Measurements from an Operational Stepped Frequency Microwave Radiometer. *Mon. Weather Rev.* **2007**, *135*, 3070-3085.
2. Ruf, C.S.; Principe, C. X-band Lightweight Rainfall Radiometer First Light. In *Proceedings of IEEE International Geoscience Remote Sensing Symposium*, Toulouse, France, July 2003.
3. El-Nimri, S.F.; Alswiss, S.; Jones, W.L.; Uhlhorn, E.; Johnson, J. Hurricane Imaging Radiometer Wide Swath Simulation for Wind Speed and Rain Rate. In *IEEE International Geoscience & Remote Sensing Symposium*, Boston, MA, USA, July 2008.
4. Holland, G.J. An Analytic Model of the Wind and Pressure Profiles in Hurricanes. *Mon. Weather Rev.* **1980**, *108*, 1212-1218.
5. Holton, J.R. *An Introduction to Dynamic Meteorology*. 3rd ed.; Academic Press: San Diego, CA, USA, 1992.
6. Bell, K.; Ray, P.S. North Atlantic Hurricanes 1977–99: Surface Hurricane-Force Wind Radii, *Amer. Meteorol. Soc.* **2004**, *132*, 1167-1189.
7. Chen, S.S.; Price, J.F.; Zhao, W.; Donelan, M.A.; Walsh, E.J. The CBLAST-Hurricane Program and the Next-Generation Fully Coupled Atmosphere-Wave-Ocean Models for Hurricane Research and Prediction. *Bull. Amer. Meteorol. Soc.* **2007**, *88*, 311-317.

© 2010 by the authors; licensee Molecular Diversity Preservation International, Basel, Switzerland. This article is an open-access article distributed under the terms and conditions of the Creative Commons Attribution license (<http://creativecommons.org/licenses/by/3.0/>).